

Functionalized 2-(hydroxyethyl) methacrylate (HEMA)-co-acrylamide (AAm) hydrogels: Kinetic and Isotherm Modelling Analysis on the Removal of Cu(II) Ions

AYÇABAL ÖZTÜRK^{1,2,*}, ZEHRA ÖZBAŞ³, BENGİ ÖZKAHRAMAN⁴ AND SERKAN EMİK⁵

1. Istinye University, Faculty of Pharmacy, Department of Analytical Chemistry, 34010, Zeytinburnu, Istanbul, Turkey
2. Istinye University, Institute of Health Sciences, Department of Stem Cell and Tissue Engineering, 34010 Istanbul, Turkey
3. Cankırı Karatekin University, Faculty of Engineering, Department of Chemical Engineering, 18200, Cankırı, Turkey
4. Hitit University, Faculty of Engineering, Department of Polymer Engineering, 19030, Corum, Turkey
5. Istanbul University-Cerrahpaşa, Faculty of Engineering, Department of Chemical Engineering, 34320, Istanbul

ABSTRACT

A functionalized hydrogel composed of 2-(hydroxyethyl) methacrylate (HEMA) and acrylamide (AAm) was synthesized by amination and saponification reactions, respectively, and its functionality was examined for the elimination of copper(II) ions. The maximum adsorption capacity for copper(II) ions was 0.617 mmol g⁻¹ before saponification, whereas it was 1.2225 mmol g⁻¹ after saponification. The adsorption data was analyzed with pseudo-first-order ($r^2=0.8867$), intra-particle diffusion ($r^2=0.9453$), Elovich ($r^2=0.9489$) and pseudo-second-order ($r^2=0.9999$) kinetic models. Based on the adsorption equilibrium experimental data Freundlich ($r^2=0.9964$), Langmuir ($r^2=0.998$) and Dubinin–Radushkevich (D-R) ($r^2=0.9960$) adsorption isotherms provided good fits for all of experimental results. Finally, the data of kinetic experiments obtained in this study showed the applicability of the functionalized gel for Copper(II) ion removal.

KEYWORDS: Aminofunctionalized gel, Saponification, Adsorption kinetics, Adsorption isotherms, Cu(II) ions removal

J. Polym. Mater. Vol. 36, No. 2, 2019, 161-173

© Prints Publications Pvt. Ltd.

Correspondence author e-mail: aycabal@gmail.com, aozturk@istinye.edu.tr

DOI : <https://doi.org/10.32381/JPM.2019.36.02.5>

INTRODUCTION

Heavy metal pollution is a worldwide issue especially for the environment and accordingly living species. Heavy metals are not biodegradable which means they cause pollution, even in very small concentrations. They are toxic or carcinogenic. Moreover, the increased concentration of heavy metal affects severely the living organisms^[1,2].

There are many conventional techniques commonly applied to extract heavy metal ions such as precipitation^[3, 4], ion exchange^[5-7], adsorption^[8-11], reverse osmosis^[12, 13], electrochemical treatments^[14-16], hyperfiltration^[17], membrane separation, evaporation, flotation^[18-20], coagulation^[14, 21], oxidation and biosorption processes^[22, 23] and others. Adsorption is an easy, relatively low-cost, and efficient method to eliminate heavy metal ions^[24-26]. So it is the preferable method for controlling of water pollution.

Hydrogels are three-dimensional cross-linked polymeric networks that can absorb a large amount of water in their swollen state because of the hydrophilic groups in their backbone. Hydrogels have attracted particular attention as adsorbent materials due to the facility of the incorporation of different chelating groups into the polymeric networks. Thus far, numerous monomers containing hydrophilic groups such as amino, hydroxyl, carboxyl, and sulfonate which can form complex with metal ions and dyes have been used to synthesize functionalized hydrogels. Their low cost and efficiency have caused attention for polyacrylamide based crosslinked polymers. Their adsorption capacities were enhanced by surface

modifications. The studies on amino-functionalized polymers concluded that high metal adsorption capacities were caused by the protonation and electrostatic interactions of the amine functions^[27-35].

This study reports an economical polymeric material for the efficient and reproducible removal of Cu(II) ion. AAm can be saponified to convert a part of $-\text{CONH}_2$ to $-\text{COO}^-$ and $-\text{COOH}$ to make carboxylate sites that present as the binding sites for heavy metal ion. For this purpose, according to a precise survey on the Chemical Abstracts, an amino-functionalized HEMA-AAm based hydrogel prepared by transamination reaction with ethylenediamine (EDA) was synthesized for the first time, and its potential use was evaluated based on elimination of copper (II) ions from aqueous solutions. Saponification of aminofunctionalized HEMA-AAm based hydrogel was carried out under alkaline conditions to increase the absorption rate significantly. The adsorption behavior of the saponificated hydrogel was compared with that of aminofunctionalized hydrogel. It can be resulted that the adsorption method was efficient, and it achieved a higher adsorption equilibrium amount of $1.2225 \text{ mmol.g}^{-1}$ in about 7 h of the process for saponificated hydrogel.

EXPERIMENTAL

Materials

Acrylamide (AAm), 2-(hydroxyethyl) methacrylate (HEMA), ethylenediamine (EDA), copper (II) acetate monohydrate were Sigma-Aldrich (St. Louis, MO) products. N, N'- methylene-bis-acrylamide (NMBA), N, N, N', N',-tetramethyl ethylenediamine (TEMED) and APS were obtained from Riedel-de Haen (Seelze, Germany). The other chemicals used were analytical purity.

Preparation of HEMA-AAm hydrogel

The synthesis of HEMA-AAm hydrogel was carried out in a glass tube (1.3 cm internal diameter × 15 cm length) by free radical chain polymerization in presence of NMBA as crosslinker. The initiator, APS and accelerator, TEMED were used for the polymerization system. First of all, desired amount of HEMA, AAm (1:1; mole ratio) and NMBA (5 % mole of monomers) were dissolved in ultrapure water to obtain 1M monomer concentration. The reaction mixture was continuously flushed with nitrogen and lastly APS and TEMED were added into the reaction tube before closing the cap. The used dose of APS and NMBA were 1 mol% of total monomer concentration, and TEMED was added with an equal weight of APS. Later on, the tube was inserted into a water-bath held at 60°C. After 24 h, the gels were removed out of the tube and they were cut into small discs in 1 cm length. The discs were rinsed with distilled water for one week to extract the impurities.

Preparation of aminofunctionalized HEMA-AAm hydrogel (A-HEMA-AAm)

To obtain aminofunctionalized gel, 1 g HEMA-AAm hydrogel and 10 g EDA were taken in a test tube and allowed at 80°C for 4 h in an inert atmosphere. The obtained gel was washed with methanol to purify and free from unreacted amine compound. The aminofunctionalized hydrogel (A-HEMA-AAm) was dried until it gets constant weight.

Saponification of aminofunctionalized HEMA-AAm hydrogel (SA-HEMA-AAm)

1g A-HEMA-AAm hydrogel was treated with 10 ml of 2M NaOH aqueous solution. After proceeding of the reaction for 2 h with stirring at 95°C, the obtained hydrogel was rinsed with deionized water till getting neutral pH. Also, the final product (SA-HEMA-AAm) was suspended in methanol, disintegrated by a blender to get fine powder. Later, it was dried under vacuum. The reaction mechanism was illustrated step-by-step in Figure 1.

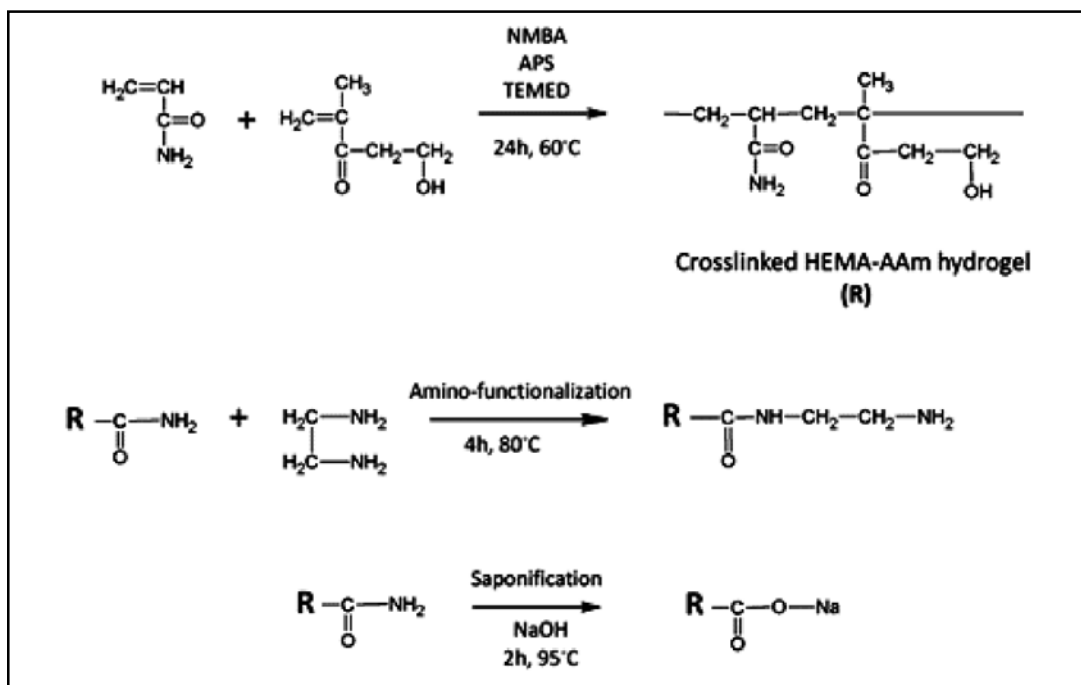


Fig. 1. The reaction mechanism.

Characterization

The structural characterization of the synthesized materials was carried out by KBr disk using a FT-IR spectrophotometer (Perkin Elmer Inc., Wellesley, MA). Nitrogen physisorption measurements of the samples were obtained by Quantachrome Nova 3200e BET surface area analyzer at -196°C . In addition, amine value of the adsorbent was determined by volumetric method described in the literature [27] and found to be 1.8 mmol g^{-1} .

Adsorption studies

The ion removal capacities of the final product (SA-HEMA-AAm) were determined using aqueous Cu(II) solution. The procedure was started by adding SA-HEMA-AAm (0.1 g) to the stock solution (100 mL) in a vial at 25°C at the agitation speed of 500 rpm and pH 4.5. The initial metal ion concentration was 250 ppm for kinetic studies, and the metal ion concentrations like 200, 250, 300, 350, 400 and 500 ppm were also taken to evaluate the adsorption isotherms. The concentrations of copper(II) heavy metal ions were determined by means of AAS (Perkin-Elmer Analyst 200 model) at certain time intervals. The equilibrium adsorption capacity of the gels was estimated by the following equation (1), q (mol g^{-1}),

$$q \left(\frac{\text{mol}}{\text{g}} \right) = \frac{(C_i - C_e) \times V}{m} \quad (1)$$

C_i : concentrations of Cu(II) metal ion in heavy metal solution (mol L^{-1}) before adsorption

C_e : concentrations of Cu(II) metal ion in heavy metal solution (mol L^{-1}) after adsorption

m : gel amount (g)

V : total volume (L)

All measurements were carried out three times, and the average value was figured on calculating adsorption studies.

RESULTS AND DISCUSSION

FT-IR and BET analysis

FT-IR spectra of the HEMA-AAm, A-HEMA-AAm and SA-HEMA-AAm are illustrated in

Figure 2. The description of the infrared spectrum of HEMA-AAm had the absorption peaks at 1653 and 1720 cm^{-1} that are ascribed to the carbonyl stretching frequency of the amide group (amide I) in the AAm unit and the ester carbonyl stretching frequency of the HEMA unit, respectively. The broad band at around 3400 cm^{-1} points out the presence of hydroxyl group and also hydrogen bonding between amide units of AAm and hydroxyl units of HEMA [36, 37]. In the spectra of aminofunctionalized HEMA-AAm, the band appeared at 1567 cm^{-1} confirms the transamidation reaction between primary amide groups and diamine [38]. The carbonyl groups of esters change to carboxylate groups by base treatment (after the saponification) in which the band ascribed to the carbonyl units of amide almost disappeared. In addition, the intensity of the absorption band around 1650 cm^{-1} decreased, whereas, the band at 1560 cm^{-1} belonging to the $-\text{COO}^-$ and $-\text{COO}^-\text{Na}^+$ groups had a moderate intensity. This peak also confirms the formation of major group of $-\text{COO}^-$ and $-\text{COO}^-\text{Na}^+$ in the network thorough saponification process [34].

The BET analysis revealed that the surface area of aminofunctionalized HEMA-AAm hydrogel (A-HEMA-AAm) was increased after saponification (SA-HEMA-AAm). The surface area is an important issue for adsorption capacity of any materials. Generally, the higher surface area means the larger adsorption capacity [39, 40]. The measured BET surface areas were 4.266 and $27.182 \text{ m}^2/\text{g}$ for A-HEMA-AAm and SA-HEMA-AAm, respectively. After saponification, the adsorption amount raised from 0.617 to 1.2225 mmol/g .

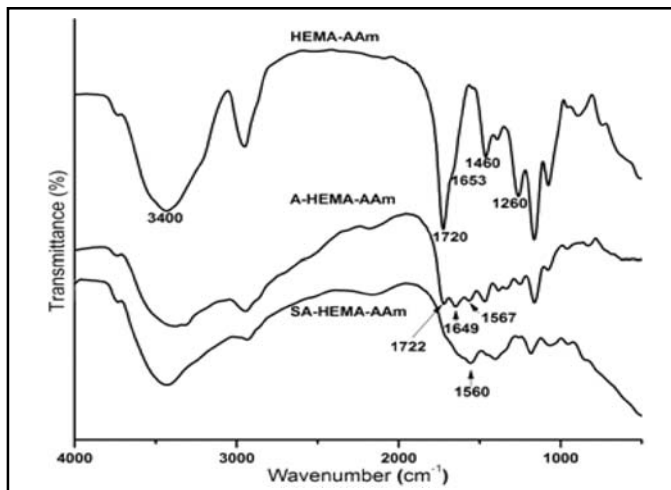


Fig. 2. FTIR spectra of HEMA-AAm gel (a) and the functionalized gels, A-HEMA-AAm (b) and SA-HEMA-AAm (c).

Adsorption kinetics

The effect of the contact time on SA-HEMA-AAm gel was performed to investigate the adsorption kinetic of Copper(II) metal ion. As seen in Figure 3, adsorption capacity showed

an increase trend with the contact time, and almost 96% of the total adsorption was completed in the first 7 h, and q (maximum adsorption amount) was observed to be $1.2225 \text{ mmol g}^{-1}$.

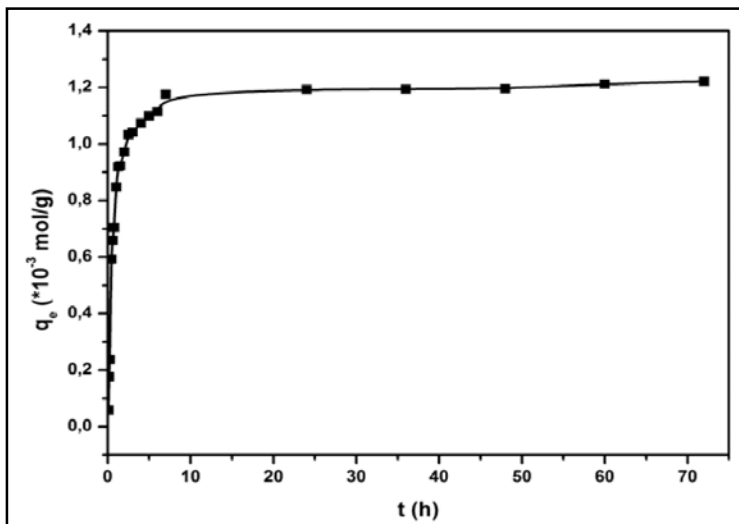


Fig. 3. Effect of contact time on the adsorption of Cu(II).

In this study, the experimental data was tested by using kinetic models such as pseudo-first-order, pseudo-second-order, Elovich and intra-particle diffusion models. The linear format pseudo-first-order model expression as given by Lagergren is presented in the equation (2)^[41]:

$$\ln(q_e - q_t) = \ln q_e - (k_1 t) \quad (2)$$

q_e : amount of Copper(II) capacity at equilibrium time (mol g⁻¹)

q_t : amount of Copper(II) capacity at a certain time t (mol g⁻¹)

By the linear plot of $\ln(q_e - q_t)$ against t, the values of k_1 (the rate constant of first order adsorption, h⁻¹) and q_e can be derived from the slope and intercept, respectively.

The pseudo-second-order kinetic model is defined as follows^[42]:

$$t/q_t = (1/k_2 q_e^2) + (t/q_e) \quad (3)$$

The values k_2 (the rate constant, g mol⁻¹ h⁻¹) and q_e could be estimated experientially by the slope and intercept of the plot of t/q_t against t.

Elovich kinetic model equation is mostly denoted as given in the equation (4)^[43]:

$$q_t = 1/\beta \ln(\alpha \beta) + 1/\beta \ln(t) \quad (4)$$

The constants, α (primary rate constant, mol g⁻¹ min⁻¹) and β (adsorption constant, g mol⁻¹) could be found out from the slope and intercept of a linear plot of q_t against $\ln(t)$.

The intra-particle diffusion model equation is generally expressed as following equation(5)^[44]:

$$q_t = k_{pi} t^{1/2} + C_i \quad (5)$$

k_{pi} (diffusion rate constant values, mol g⁻¹ h^{-1/2}) and C_i (adsorption constant, mol g⁻¹) values could be figured out by the intercept and slope of the linear line of q_t against $t^{1/2}$, respectively.

According to Table 1, it can be considered that the coefficient of correlation was 0.8867 for the pseudo-first-order model, and the discrepancy between the theoretical $q_{e,teo}$ and experimental $q_{e,exp}$ rates were huge. Thus, pseudo-first-order kinetic model are not suited to define the adsorption process. On contrary, the high

TABLE 1. Calculated adsorption parameters for different kinetic models.

Kinetic models		$q_{t,exp}$ (*10 ⁻³ mol g ⁻¹) 1.2225	
Pseudo-first-order constant	k_1 (min ⁻¹) 0.0065	$q_{e,teo}$ (*10 ⁻³ mol g ⁻¹) 0.7263	r^2 0.8867
Pseudo-second-order constant	k_2 (*10 ³ g mol ⁻¹ min ⁻¹) 0.0203	$q_{e,teo}$ (*10 ⁻³ mol g ⁻¹) 1.2261	r^2 0.9999
Intra-particle diffusion constant	k_3 (*10 ⁻³ mol g ⁻¹ min ^{-1/2}) 0.0200	C_3 (*10 ⁻³ mol g ⁻¹) 0.7587	r^2 0.9453
Elovich constant	β (*10 ³ g mol ⁻¹) 3.8109	α (*10 ⁻³ mol g ⁻¹ min ⁻¹) 0.0748	r^2 0.9489

correlation coefficient value (0.9998) and the compatibility between the $q_{e,exp}$ and $q_{e,theo}$ data make pseudo-second-order model more appropriate than others (Figure 4). As

understood from Table 1, the correlation coefficient for Elovich equation was 0.9489, and the experimental value showed poor agreement of Elovich kinetic model.

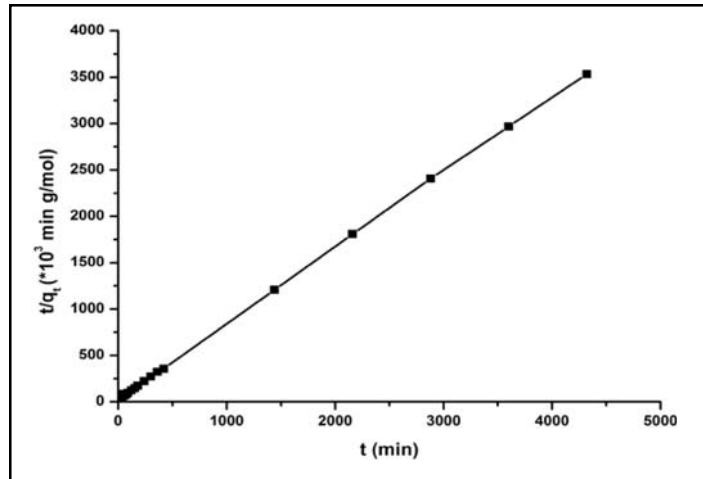


Fig. 4. The pseudo-second order kinetic plot

The intra-particle diffusion model was developed by Weber and Morris, to identify the adsorption behavior, which affects the adsorption kinetics by fitting to the kinetic experimental data. An

adsorption process fits the intra-particle diffusion mechanism only if the plot of q versus $t^{1/2}$ is linear, and it passes from the origin.

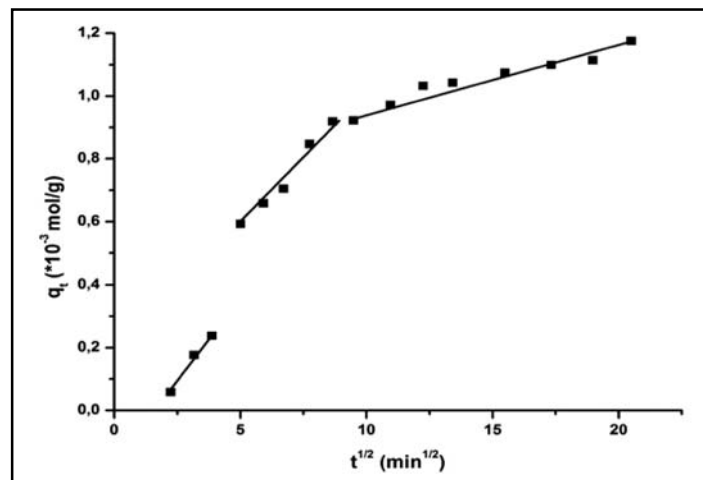


Fig. 5. Intra-particle diffusion kinetic plot.

As presented in Figure 5, the multi-linear plot showed that the adsorption mechanism consists of three stages; (i) the beginning phase was the exterior surface adsorption, (ii) the second phase was the stepped adsorption because of the intra-particle or pore diffusion, (iii) the third phase was ascribed to the final equilibrium phase [45, 46, 47].

The $q_{e,cal}$ value was calculated close to the experimental one ($t=24\text{ h } q_{e,cal}=1.23 \cdot 10^{-3} \text{ mol g}^{-1}$), and the intercept values (C) weren't zero nevertheless C_3 was larger than C_1 and C_2 . In addition, the intra-particle diffusion rate, k_{p2} was lower than the external mass diffusion rate, k_{p1} . As shown, the process possessed different adsorption phases, so the rate-controlling stage can be determined by the equation (6) [48]:

$$F = q_t/q_\infty = 1 - \frac{6}{\pi^2} \sum_{n=1}^{\infty} (1/n^2) \exp(-n^2 B_t) \quad (6)$$

q_t : adsorption capacity at certain time t (mol g^{-1})

q_∞ : adsorption capacity at infinite time (mol g^{-1})

B_t : mathematical use of F

n : Freundlich constant

The kinetic expression can be formed as the equations (7) and (8) [49]:

for $0 \leq f \leq 0.85$

$$B_t = 2\pi - (\pi^2 F/3) - 2\pi(1 - \pi F/3)^{1/2} \quad (7)$$

for $0.86 \leq f \leq 1$ and

$$B_t = -\ln(1 - F) - 0.4977 \quad (8)$$

B_t were calculated for each value of F by equation (7) and (8). As seen from Figure 6, the plot between B_t vs t is linear, and the linear plot demonstrates the controlling adsorption mechanism. If the linear plot gets through the

origin, intra-particle diffusion is dominated on adsorption, whereas, if the plot is not linear to pass the origin, the mechanism is controlled by external mass diffusion. As seen from Figure 6, the low linearity of the plots and not getting through the origin make the external mass diffusion dominated than the intra-particle diffusion.

Adsorption isotherms

The relevance between the adsorption amount on the sorbent material and the concentration of the dissolved adsorbate in solution at equilibrium was defined as adsorption isotherm. In presented study, the relevance of the primary copper(II) ion concentration (C_e) on the adsorbed copper (II) amount (q_e) was given in Figure 7. As seen, q_e value increased with the increasing initial concentration of Copper(II) ion.

To optimize the adsorption process of Copper(II) ion on saponificated amino functionalized HEMA-AAm gel, the kinetic data was tested by Langmuir, Freundlich, and D-R isotherm models. The linearized equations (9), (10) and (11) of the isotherm models is stated as:

Langmuir isotherm equation is given by [50]:

$$C_e/q_e = 1/b q_{max} + C_e/q_{max} \quad (9)$$

q_e : equilibrium adsorption capacity per gram on the adsorbent (mol g^{-1})

C_e : equilibrium concentration of Copper(II) metal ion (mol L^{-1})

q_{max} : maximum amount of the adsorbent monolayer the surface (mol g^{-1})

b : Langmuir constant (L mol^{-1})

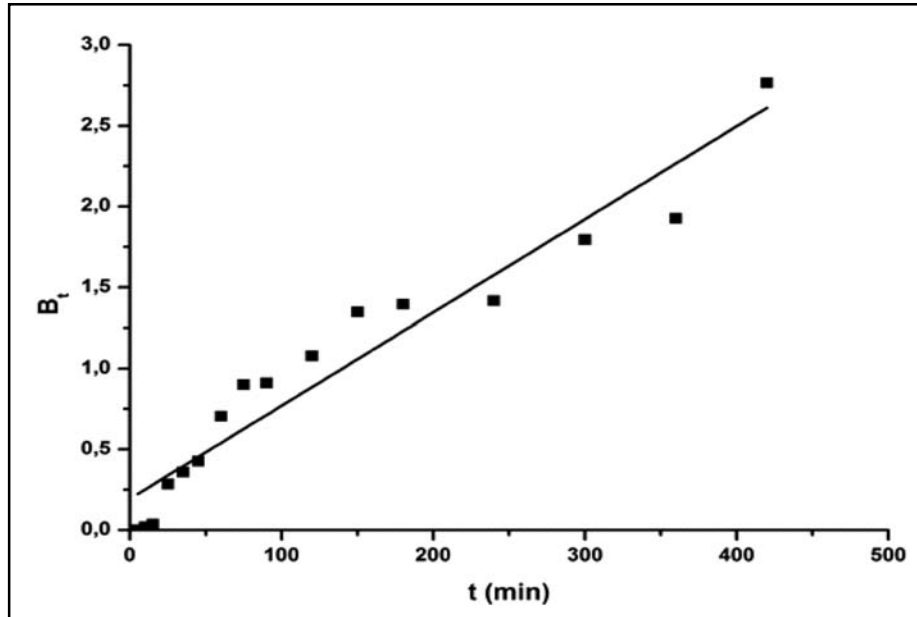


Fig. 6. Linearity between B_t against t .

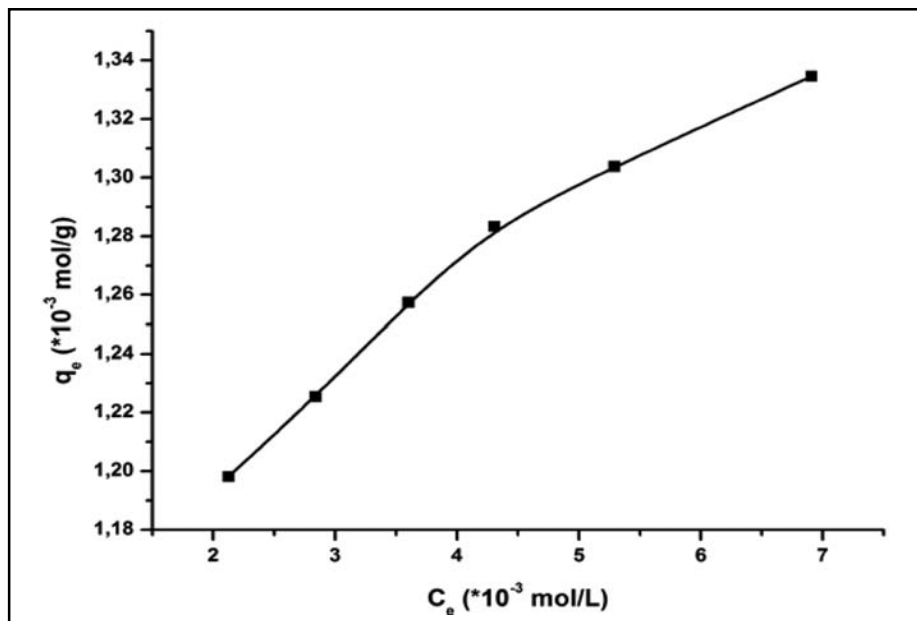


Fig. 7. Effect of initial metal ion concentration

Freundlich isotherm equation is given by^[51]:

$$\ln q_e = \ln K_f + \frac{1}{n} \ln C_e \quad (10)$$

n : exponent of the Freundlich equation,

K_f : Freundlich constant.

D-R isotherm equation is given by^[52]:

$$\ln q_e = \ln q_m - \beta \varepsilon^2 \quad (11)$$

q_m : monolayer (max.) adsorption capacity (mol g⁻¹)

β : activity coefficient

ε : Polanyi potential,

$$\varepsilon = RT \ln (1 + 1/C_e) \quad (12)$$

The constant (β) supplies the mean free-energy (E_a) for sorption per mole of adsorbent as it is transmitted to the solid surface from infinity in the heavy metal solution, and it is represented by^[54]:

$$E_a = (2\beta)^{-1/2} \quad (13)$$

The Langmuir isotherm indicates monolayer surface adsorption by uniform energies at active sites. As seen from Table 2, the r^2 value is > 0.99 that indicates a very good mathematical fit, and it signs the monolayer adsorption of the ion at given temperature^[54, 55].

TABLE 2. Isotherm constant values.

Isotherms		Constants		
Langmuir	q_{max} b (*10 ³ L mol ⁻¹) 1.41	(*10 ⁻³ mol g ⁻¹) 2.416		r^2 0.998
Freundlich	K_f (*10 ³ mol ^{1-1/n} L ^{1/n} g ⁻¹) 2.13	1/n 0.0937		r^2 0.9964
D-R	q_m (*10 ⁻³ mol g ⁻¹) 1.65	β (*10 ⁻³ mol ² kJ ⁻²) 0.0014	E_a (kJ mol ⁻¹) 18.90	r^2 0.9960

The Freundlich isotherm model is depend on the heterogeneous surface adsorption with non-uniform energies of active site. The value of $1/n < 1$ (Table 2) implies that the adsorption capacity is lightly suppressed at lower equilibrium concentrations which means multilayer adsorption of Copper(II) ion on the surface^[56-59].

The D–R isotherm gives knowledge on adsorption mechanism of adsorbate onto adsorbent. If E_a is higher than 8 kJ mol⁻¹, it

represents chemical adsorption, while if E_a is lower than 8 kJ mol⁻¹, it means physical adsorption^[60]. As E value is 18.9 kJ mol⁻¹, it implies that adsorption process is controlled by chemical adsorption.

In conclusion, the correlation coefficients were high and closer to 1 for all isotherm models (Table 2 and Figure 8), and this states that the adsorption on the surface adsorbent could be clarified by using any of these isotherm models.

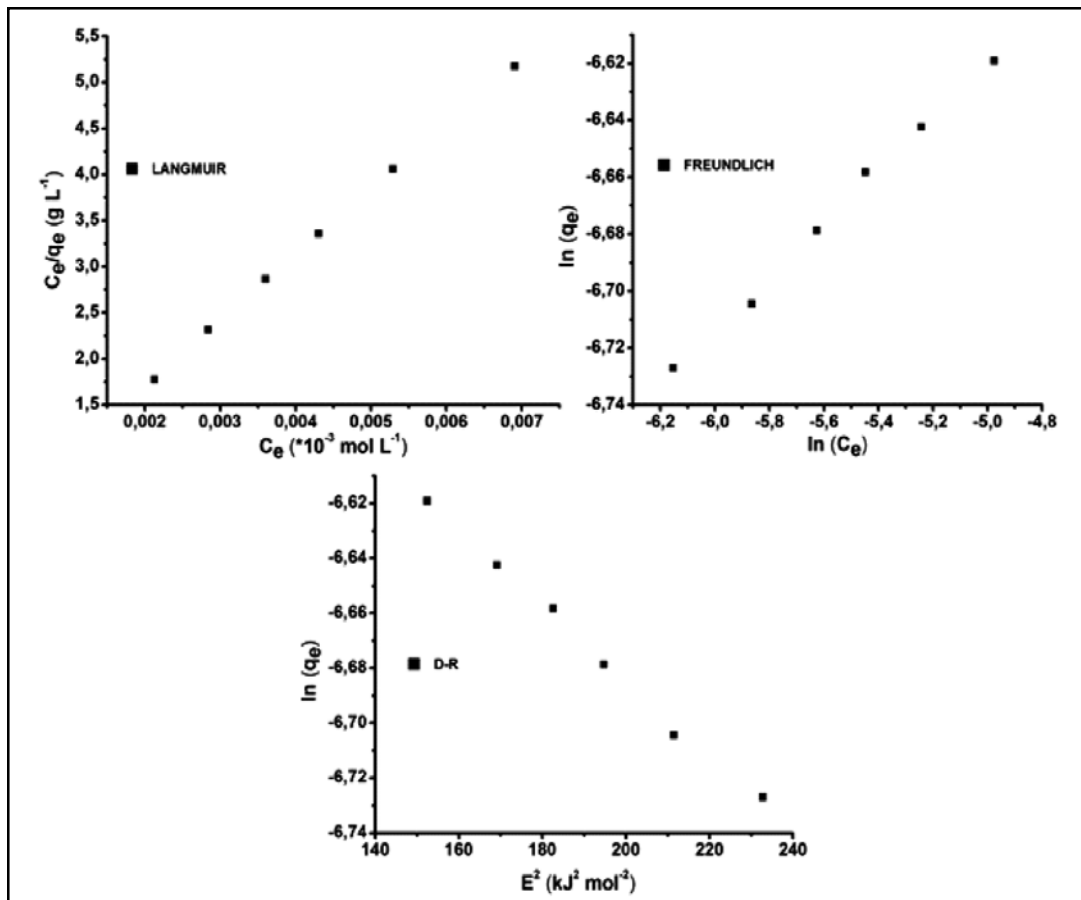


Fig. 8. Langmuir, Freundlich, and D-R plots for the adsorption of Cu(II) ion.

CONCLUSIONS

In this investigation, the synthesis and metal ion adsorption capacity synthesized gel (SA-HEMA-AAm) was examined using copper(II) ion. The synthesis of functionalized HEMA-AAm hydrogel was proved by FTIR analysis. The confirmation of transamidation and saponification reactions of HEMA-AAm gel was obtained by the bands at 1567 and 1540 cm^{-1} , respectively. In addition, after the saponification

reaction, surface area as well as adsorption capacity of the gel was improved. The adsorption performance improved with the increase in the contact time and the concentration of primary metal ion. The adsorption equilibrium of copper (II) was observed to reach in 7 h. The kinetic adsorption studies emerged that adsorption profiles of the gel followed pseudo-second order kinetic model, and external mass diffusion mechanism can be effectively used on adsorption. The

equilibrium analysis displayed that the used isotherm models well-suited to the experimental value. Conforming to the increased adsorption amount, the functionalized gel may have potential usage of adsorption of heavy metal Copper(II) ion for wastewater purification.

ACKNOWLEDGEMENTS

This research was financially supported by the Research Fund of Istanbul University, (Project No: 22058 and 37685).

REFERENCES

- 1 A. Dabrowski, Z. Hubicki, P. Podkoscielny, E. Robens, *Chemosphere*, **56(2)** (2004) 91
- 2 F. Fu, Q. Wang, *J. Environ. Manage.*, **92(3)** (2011) 407
- 3 Q. Chen, Z. Luo, C. Hills, G. Xue, M. Tyrer, *Water Res.*, **43(10)** (2009) 2605
- 4 A. Ozverdi, M. Erdem, *J. Hazard. Mater.*, **137(1)** (2006) 626
- 5 S. Y. Kang, J. U. Lee, S. H. Moon, K. W. Kim, *Chemosphere*, **56(2)** (2004) 141
- 6 B. Alyüz, S. Veli, *J. Hazard. Mater.*, **167(1-3)** (2009) 482
- 7 I. C. Ostroski, M.A.S.D. Barros, E.A. Silva, J. H. Dantas, P.A. Arroyo, O. C. M. Lima, *J. Hazard. Mater.*, **161(2-3)** (2009) 1404
- 8 K. C. Kang, S. S. Kim, J. W. Choi, S. H. Kwon, *J. Ind. Eng. Chem.*, **14(1)** (2008) 131
- 9 H. G. Park, T. W. Kim, M. Y. Chae, I. K. Yoo, *Process Biochem*, **42(10)** (2007) 1371
- 10 K. Pillay, E. M. Cukrowska, N.J. Coville, *J. Hazard. Mater.*, **166(2-3)** (2009) 1065
- 11 M. I. Kandah, J. L. Meunier, *J. Hazard. Mater.*, **146(1-2)** (2007) 283
- 12 M. Mohsen-Nia, P. Montazeri, H. Modarress, *Desalination.*, **217(1-3)** (2007) 276
- 13 E. Dialynas, E. Diamadopoulos, *Desalination.*, **238(1-3)** (2009) 302
- 14 G. Chen, *Sep. Purif. Techno L.*, **38(1)** (2004) 11
- 15 I. Kabdasli, T. Arslan, T. Olmez-Hancý, I. Arslan-Alaton, O. Tunay, *J. Hazard. Mater.*, **165(1-3)** (2009) 838
- 16 T. Ölmez, *J. Hazard. Mater.*, **162(2-3)** (2009) 1371
- 17 S. Chen, Y. Zou, Z. Yan, W. Shen, S. Shi, X. Zhang, H. Wang, *J. Hazard. Mater.*, **161(2-3)** (2009) 1355
- 18 M. Lundh, L. Jonsson, J. Dahlquist, *Water Research.*, **34(1)** (2000) 21
- 19 H. Polat, D. Erdogan, *J. Hazard. Mater.*, **148(1-2)** (2007) 267
- 20 X. Z. Yuan, Y. T. Meng, G. M. Zeng, Y. Y. Fang, J. G. Shi, *Colloids. Surf. A*, **317(1-3)** (2008) 256
- 21 Q. Chang, G. Wang, *Chem. Eng. Sci.*, **62(17)** (2007) 4636
- 22 W. L. Yan, R. Bai, R., *Water Research.*, **39(4)** (2005) 688
- 23 X. Liu, Q. Hu, Z. Fang, X. Zhang, B. Zhang, *Langmuir.*, **25(1)** (2009) 3
- 24 W. S. Wan Ngah, C. S. Endud, R. Mayanar, *React. Funct. Polym.*, **50(2)** (2002) 181
- 25 S. S. Banerjee, D. H. Chen, *J. Hazard. Mater.*, **147(3)** (2007) 792
- 26 Y. H. Li, Z. Di, J. Ding, D. Wu, Z. Luan, Y. Zhu, *Water Research.*, **39(4)** (2005) 605
- 27 H. Kasgoz, S. Ozgumus, M. Orbay, *Polymer*, **44(6)** (2003) 1785
- 28 H. Chen, A. Wang, *J. Hazard. Mater.*, **165(1-3)** (2009) 223
- 29 H. Kasgoz, *Polym. Bull.*, **56** (2006) 517
- 30 N. Wu, Z. Li, *Chem. Eng. J.*, **(215-216)** (2013) 894

- 31 S. E. Bailey, T. J. Olin, R. M. Bricka, D. D. Adrian, *Water Research.*, **33(11)** (1999) 2469
- 32 T. S. Anirudhan, P. S. Suchithra, S. Rijith, S., *Colloid Surf. A*, **326(3)** (2008) 147
- 33 G. S. Chauhan, S. Chauhan, U. Sen, D. Garg, *Desalination*, **243(1-3)** (2009) 95
- 34 S. P. Shukla, S. Devi, *Process Biochem.*, **40(1)** (2005) 147
- 35 K. Kesenci, R. Say, A. Denizli, *Eur. Polym. J.*, **38(7)** (2002) 1443
- 36 M. Rapado, C. Peniche, *Polimeros.*, **25(6)** (2015) 547
- 37 M. Babazadeh, *J. Applied Polym. Sci.*, **104(4)** (2007) 2403
- 38 H. Kasgoz, *Colloid Surf. A.*, **266(1-3)** (2005) 44
- 39 H. El-Hamshary, M. M. G. Fouda, M. Moydeen, S. S. Al-Deyab, S.S., *Int. J. Biol. Macromol.*, **66** (2014) 289
- 40 B. Özkahraman, *J. Polym. Environ.*, **26(3)** (2018) 1113.
- 41 S. Lagergren, *Kungliga Svenska Vetenskapsakademiens Handlingar*, **24(4)** (1898) 1
- 42 Y. S. Ho, G. McKay, *Process Biochem.*, **34(5)** (1999) 451
- 43 S. H. Chien, W. R. Clayton, *Soil Sci. Soc. of Am. J.*, **44(2)** (1980) 265
- 44 W. J. Weber, J. C. Morris, *J. Sanit. Eng. Div.*, **89(2)** (1963) 31
- 45 F. C. Wu, R. L. Tseng, R. S. Juang, *Chem. Eng. J.*, **153(1-3)** (2009) 1
- 46 Z. Ozbas, C. P. Sahin, E. Esen, G. Gurdag, H. Kasgos, *J. Environ. Chem. Eng.*, **4** (2016) 1948
- 47 A. E. Ofomaja, *Bioresour. Technol.*, **101(15)** (2010) 5868
- 48 G. E. Boyd, A. W. Adamson, L. S. Myers, *J. Am. Chem. Soc.*, **69**(1947) 2836
- 49 D. Reichenberg, *J. Am. Chem. Soc.*, **75** (1953) 589
- 50 I. Langmuir, *J. Am. Chem. Soc.*, **40** (1918) 1361
- 51 H. M. F. Freundlich, *J. Phys. Chem.*, **57** (1906) 385
- 52 M. M. Dubinin, L. V. Radushkevich, *Proceedings of the Academy of Sciences of the USSR, Physical Chemistry Section*, **55**(1947) 331
- 53 J. P. Hobson, *J. Phys. Chem.*, **73**(1969) 2720
- 54 J. P. Laurino, *J. Macromol. Sci. Pure Appl. Chem.*, **45(8)** (2008) 612
- 55 O. Moradi, K. Zare, M. Monajjemi, M. Yari, H. Aghaie, *Fuller. Nanotub. Car. N*, **18(3)** (2010) 285
- 56 N. A. Ismail, S. Bakhshaei, M. A. Kamboh, N. S. Abdul Manan, S. Mohamad, M. Yilmaz, *J. Macromol. Sci. Pure Appl. Chem.*, **53(10)** (2016) 619
- 57 S. Parlayıcı, V. Eskizeybek, A. Avcý, E. Pehlivan, *J. Nanostructure Chem.*, **5(3)** (2015) 255
- 58 S. Kubilay, R. Gürkan, A. Savran, T. Sahan, *Adsorption*, **13(1)** (2007) 41
- 59 A. Bal, B. Özkahraman, I. Acar, M. Özyürek, G. Güçlü, *Desalin Water Treat.*, **52(16-18)** (2014) 3246
- 60 H. Ren, Z. Gao, D. Wu, J. Jiang, Y. Sun, C. Luo, *Carbohydr. Polym.*, **137** (2016) 402

Received: 10-05-2019

Accepted: 04-06-2019